Physics Letters B 809 (2020) 135702

Contents lists available at ScienceDirect

Physics Letters B

www.elsevier.com/locate/physletb

Benchmarking ^{136}Xe neutrinoless $\beta\beta$ decay matrix element calculations with the ^{138}Ba(p,t) reaction

B.M. Rebeiro [a], S. Triambak [a,*], P.E. Garrett [b,a], B.A. Brown [c], G.C. Ball [d], R. Lindsay [a], P. Adsley [e,f], V. Bildstein [b], C. Burbadge [b], A. Diaz Varela [b], T. Faestermann [g], D.L. Fang [h,i], R. Hertenberger [j], M. Horoi [k], B. Jigmeddorj [b], M. Kamil [a], K.G. Leach [l], P.Z. Mabika [a,m], J.C. Nzobadila Ondze [a], J.N. Orce [a], H.-F. Wirth [j]

[a] Department of Physics and Astronomy, University of the Western Cape, P/B X17, Bellville 7535, South Africa
[b] Department of Physics, University of Guelph, Guelph, Ontario N1G 2W1, Canada
[c] Department of Physics and Astronomy and National Superconducting Cyclotron Laboratory, Michigan State University, East Lansing, MI 48824-1321, USA
[d] TRIUMF, 4004 Wesbrook Mall, Vancouver, British Columbia V6T 2A3, Canada
[e] School of Physics, University of the Witwatersrand, Johannesburg 2050, South Africa
[f] iThemba LABS, P.O. Box 722, Somerset West 7129, South Africa
[g] Physik Department, Technische Universität München, D-85748 Garching, Germany
[h] Institute of Modern Physics, Chinese Academy of Sciences, Lanzhou, 730000, China
[i] School of Nuclear Science and Technology, University of Chinese Academy of Sciences, Beijing 100049, China
[j] Fakultät für Physik, Ludwig-Maximilians-Universität München, D-85748 Garching, Germany
[k] Department of Physics, Central Michigan University, Mount Pleasant, MI 48859, USA
[l] Department of Physics, Colorado School of Mines, Golden, CO 80401, USA
[m] Department of Physics and Engineering, University of Zululand, Private Bag X1001, KwaDlangezwa 3886, South Africa

ARTICLE INFO

Article history:
Received 20 April 2020
Received in revised form 16 August 2020
Accepted 16 August 2020
Available online 19 August 2020
Editor: B. Betram

Keywords:
Neutrinoless double beta decay
Nuclear matrix elements
Transfer reactions
Shell model
QRPA

ABSTRACT

We used a high-resolution magnetic spectrograph to study neutron pair-correlated 0^+ states in ^{136}Ba, produced via the ^{138}Ba(p,t) reaction. In conjunction with state-of-the-art shell model calculations, these data benchmark part of the dominant Gamow-Teller component of the nuclear matrix element (NME) for ^{136}Xe neutrinoless double beta ($0\nu\beta\beta$) decay. We demonstrate for the first time an evaluation of part of a $0\nu\beta\beta$ decay NME by use of an experimental observable, presenting a new avenue of approach for more accurate calculations of $0\nu\beta\beta$ decay matrix elements.

The massive nature of neutrinos leads to a violation of the γ_5 invariance [1] for weak interactions. Consequently, there is substantial interest worldwide [2–4] to search for standard-model-forbidden neutrinoless double beta ($0\nu\beta\beta$) decays, that violate lepton number conservation by 2 units. The observation of such decays would prove that the electron neutrino (ν_e) is a Majorana fermion, and therefore indistinguishable from its antiparticle ($\bar{\nu}_e$). This is consistent with most theories beyond the Standard Model [5], that attribute the smallness of neutrino masses to a violation of total lepton number at an energy scale of $\sim 10^{15}$ GeV [3,5].

If the mechanism driving a $0\nu\beta\beta$ decay is via the exchange of a light left-handed Majorana neutrino, then the decay amplitude is proportional to

$$m_{ee}M^{0\nu} = \left|\sum_j |U_{ej}|^2 e^{i\alpha_j} m_j\right| M^{0\nu}, \tag{1}$$

where m_{ee} is the effective Majorana mass of the electron neutrino and $M^{0\nu}$ is the nuclear matrix element (NME) for the decay. The NME is expressed as the sum of Gamow-Teller (GT), Fermi (F) and Tensor (T) components

$$M^{0\nu} = M^{0\nu}_{GT} - \left(\frac{g_V}{g_A}\right)^2 M^{0\nu}_F + M^{0\nu}_T, \tag{2}$$

* Corresponding author.
E-mail address: striambak@uwc.ac.za (S. Triambak).

https://doi.org/10.1016/j.physletb.2020.135702

Table 1
Some recent evaluations of the NME for ^{136}Xe $0\nu\beta\beta$ decay using different theoretical approaches.[a].

Method	$M^{0\nu}$
Deformed WS-QRPA (Jilin-Tübingen-Bratislava) [20]	1.11
pnQRPA (Jyväskylä) [21]	2.91
Deformed Skyrme-HFB-QRPA (Chapel Hill) [22]	1.55
Spherical QRPA (Bratislava-Tübingen-CalTech) [23]	2.46
ISM (Strasbourg-Madrid) [24]	2.19
ISM (Michigan) [12]	1.46
CDFT [25]	4.24
NREDF [26]	4.77
IBM-2 [27]	3.05
GCM [28]	2.35

[a] These results are for light Majorana neutrino exchange, with an unquenched value for the weak axial-vector coupling constant g_A.

where the Gamow-Teller contribution is the dominant term. In Eq. (1), the U_{ej} are elements of the Pontecorvo-Maki-Nakagawa-Sakata (PMNS) neutrino mixing matrix [6,7], the m_j's are the light neutrino masses and the α_j's are phases in the mixing matrix. For the special case of three-neutrino mixing, the PMNS matrix is parameterized in terms of three mixing angles and one Dirac and two Majorana CP-violating phases [2]. It is evident from Eq. (1) that in addition to the observation of a $0\nu\beta\beta$ decay process, it is also equally important to determine its half-life, which would establish the absolute neutrino mass scale. Furthermore, such a measurement also has the potential to identify the correct neutrino mass spectrum [8] and find extra sources of CP-violation in the leptonic sector [9]. However, achieving the above (or placing stringent constraints on any new physics) requires an accurate evaluation of the NME for the decay. This has been at the forefront of nuclear physics research in recent times, with several approaches being used to calculate the NMEs for $0\nu\beta\beta$ decay candidates [10,11]. Depending on the method used, the calculations for specific isotopes disagree with one another, differing by factors of three or more in many cases [10,11]. These discrepancies result in large uncertainties for the NMEs, which not only limit the physics that can be addressed, but also the planning and execution of future $0\nu\beta\beta$ decay experiments [11]. In contrast, the NMEs for the rare (yet standard-model-allowed) two-neutrino double beta ($2\nu\beta\beta$) decays can be extracted directly from measured half-lives. These and other experimentally derived spectroscopic information have played a critical role in constraining various NME calculations [12–17].

One of the most promising candidates for observing $0\nu\beta\beta$ decays is $^{136}\text{Xe} \xrightarrow{\beta\beta} {}^{136}\text{Ba}$. Its $2\nu\beta\beta$ decay half-life is much longer than most other cases [18]. As a result, the ratio of the $0\nu\beta\beta$ decay signal to the irreducible $2\nu\beta\beta$ decay background in the vicinity of the decay endpoint energy is expected to be larger for this particular case. In fact, a highly sensitive search for $0\nu\beta\beta$ decays was recently reported for ^{136}Xe by the KamLAND-Zen collaboration [19], who placed the most stringent upper limits to date on the effective neutrino mass, with $m_{ee} < 61 - 165$ meV, depending on the choice of NME used.

We list some recent evaluations of $M^{0\nu}$ for ^{136}Xe $\beta\beta$ decay in Table 1. While some of these results are in reasonable agreement with each other, there still exist large discrepancies in the calculated values, depending on the method used. Needless to say, this is a pressing issue as future ^{136}Xe $0\nu\beta\beta$ decay experiments aim to improve their sensitivity by at least one order of magnitude [29]. Additionally, next generation experiments also intend to use the method of barium ion tagging [30] in xenon time projection chambers (TPCs). This technique has the potential to reduce room background contributions to insignificant levels, which undoubtedly would further enhance the sensitivity of ^{136}Xe $0\nu\beta\beta$ decay experiments over other experimental searches.

Finally, it is expected that due to these advantages, future ^{136}Xe $\beta\beta$ decay experiments would also place the tightest constraints on possible CP-violating Majorana phases in the PMNS matrix [31]. The phases in the neutrino mixing matrix are potential leptogenesis parameters that may explain the observed baryon asymmetry in the universe [32–34].

Due to the several reasons listed above, the $0\nu\beta\beta$ decay of ^{136}Xe presents a compelling case to address the accuracy in its calculated NME. Two methods that have been traditionally used to calculate $0\nu\beta\beta$ decay NMEs are the interacting shell model (ISM) and the quasiparticle random phase approximation (QRPA). Unlike the latter, the shell model calculations use a limited configuration space that is comprised of relatively fewer single-particle states in the vicinity of the Fermi surface. Despite this restriction, large-scale ISM calculations allow arbitrarily complex correlations between the valence nucleons. On the other hand, the QRPA calculations make use of a much larger model space with comparatively simpler configurations. In general, the ISM calculations are known to yield smaller values of $M^{0\nu}$, compared to the QRPA [2,11]. This discrepancy has been attributed to different approaches in treating the pairing (or seniority) structure of the nuclear wavefunctions [24,35]. For the most part, previous QRPA calculations assumed spherical ground states for the parent and daughter nuclei, wherein the pairing correlations between like nucleons were taken into account using the Bardeen-Cooper-Schrieffer (BCS) approximation [2,11]. It was only recently that deformed QRPA NME calculations were performed for $0\nu\beta\beta$ decays [20,22], whose results for ^{136}Xe are listed in Table 1. Compared to the spherical QRPA [21], the deformed calculations yield smaller values for the NME, and are in reasonable agreement with the ISM results. The authors of Refs. [20,22] point out that the suppression of the NME in their calculations is mainly due to differences in the pairing content of the initial and final mean fields. Unlike the spherical QRPA, the deformed calculations accounted for the sharp neutron Fermi surface in ^{136}Xe due to the neutron number $N = 82$ shell closure. This curtails the overlap between the BCS wavefunctions and leads to a significant reduction in the calculated NMEs [20,22]. The calculations also suggest that the NME can be even more suppressed if the parent and daughter nuclei have different deformations. Such a scenario will either further reduce [20,22] the QRPA overlap factors mentioned above or result in a similar seniority mismatch between the ISM wavefunctions, due to high-seniority[1] components introduced by the deformation. In comparison, the NME calculations using other many-body approaches such as the non-relativistic energy density functional (NREDF) theory, covariant density functional theory (CDFT), the interacting boson model (IBM-2) or the generator coordinate method (GCM), predict higher values for the NME (Table 1). It has been suggested that these values are most likely overestimated, because of the omission of both collective as well as non-collective correlations, depending on the calculation [11,28,36,37].

In light of the above, precise experimental information elucidating the properties of ^{136}Xe and ^{136}Ba nuclei are crucial to benchmark the NME calculations and further reduce their model dependence. Indeed, differences in the valence nucleon occupancies for these nuclei were recently determined using one nucleon transfer reactions [38,39]. Furthermore, the ground state of ^{136}Ba is not expected to have a nearly spherical structure as ^{136}Xe or ^{138}Ba. The even barium isotopes in the $N \leq 82$ region are known to be transitional, displaying a structural evolution from spherical to γ-soft behavior with decreasing neutron number [40–42]. In this Letter we discuss neutron pairing correlations in ^{136}Ba, stud-

[1] The seniority quantum number labels the number of unpaired nucleon states in a nucleus [24,35].

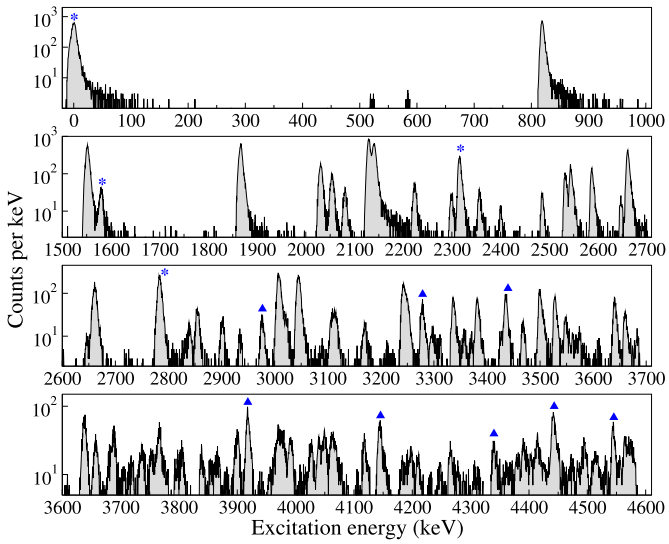

Fig. 1. Excitation energy spectrum in ^{136}Ba obtained at $\theta_{lab} = 25°$. Previously known 0^+ states are marked with asterisks, while the new 0^+ states observed in this work are shown with filled triangles.

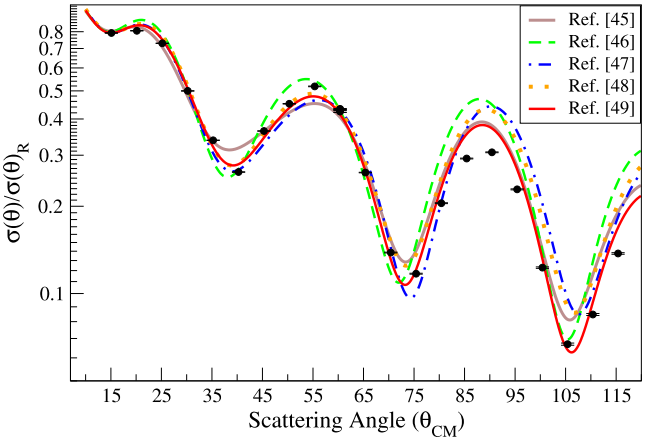

Fig. 2. Measured ^{138}Ba(p, p) angular distribution from this work (expressed in terms of ratio to the Rutherford cross sections) compared to various DWBA predictions based on different global OMP parameters.

ied with the ^{138}Ba(p, t) reaction. The experiment was performed at the Maier-Leibnitz-Laboratorium (MLL) in Garching, Germany, where a 1.5 μA, 23 MeV proton beam from the MLL tandem accelerator was incident onto a 40 μg/cm^2 thick, 99.9% isotopically enriched ^{138}BaO target, that was evaporated on a 30 μg/cm^2 carbon backing. The light reaction ejectiles were momentum analyzed using the high-resolution Q3D magnetic spectrograph [43,44], whose solid angle acceptance ranged from $2.3 - 14.6$ msr during various stages of the experiment. The detector placed at the focal plane of the Q3D spectrograph consisted of two gas proportional counters and one 7-mm-thick plastic scintillator [44]. A cathode strip foil in the second proportional counter provided position information (with a resolution of ~ 0.1 mm), while the energy losses in the gas counters and the residual energy deposited in the scintillator allowed for particle identification. The integrated beam intensity was determined using a Faraday cup that was placed at 0° to the beam, and connected to a Brookhaven Instruments Corporation (BIC) current integrator.

For our measurements, we obtained triton angular distributions using four magnetic field settings and at ten spectrograph angle settings, ranging from $\theta_{lab} = 5°$ to 50°. Fig. 1 shows sample triton spectra obtained from this experiment, where we observe states in ^{136}Ba up to ~ 4.6 MeV in excitation energy. The energy resolution of the triton peaks were found to be $\lesssim 10$ keV. We also took additional ^{138}Ba(p, p) elastic scattering data over an angular range of $\theta_{lab} = 15°$ to 115°, in 5° steps. These data were used to determine both the effective areal density of the ^{138}Ba target nuclei, as well as the appropriate global optical model potential (OMP) parameters for the incoming ^{138}Ba $+ p$ reaction channel [45–49]. The latter were used in a zero-range distorted wave Born approximation (DWBA) analysis of our data, for which we first used the DWUCK4 code [50] with Woods-Saxon potentials. As shown in Fig. 2, based on a comparison of various DWBA calculations with our elastic scattering measurements, we chose the global proton OMP parameters recommended by Varner et al. [49] for the incoming (proton) channel. For the outgoing ^{136}Ba $+ t$ channel we used the OMP parameters provided by Li et al. [51], as they gave the best agreement with our measured triton angular distribution for the ground state in ^{136}Ba (cf. Fig. 3). The transfer form factor was calculated assuming a single-step pick up of a di-neutron in a singlet relative s-state. For the core-2n coupling we used the global

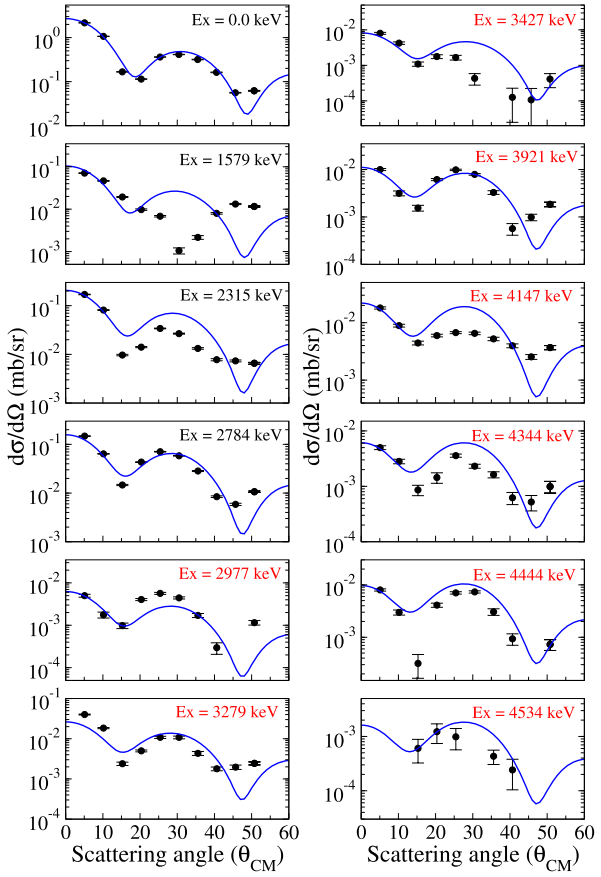

Fig. 3. Angular distributions of 0^+ states identified in this work. The solid curves are normalized DWUCK4 DWBA predictions for $L = 0$ transfer, assuming a $(0h_{11/2})^2$ configuration [39] for the form factor. The newly identified 0^+ states observed in this work are labeled in red.

OMP from Ref. [52], whose well depth was adjusted to reproduce the binding energy of each neutron [53].

The above approach was used to perform a comprehensive analysis of the angular distributions for all the triton peaks shown in Fig. 1. We defer a detailed discussion on the analysis to a forthcoming article [54]. In this Letter we only focus on the $L = 0$ angular distributions, which are critical for studying pair-correlated states in even-even nuclei. Our measured angular distributions

Table 2
Measured cross sections at $\theta_{lab} = 5^\circ$ and relative (p,t) strengths obtained from the data shown in Fig. 3.

E_x [keV]	$(d\sigma/d\Omega)_{5^\circ}$ [mb/sr]	ϵ_i [%]
0	2.17(12)	100.0
1579	0.071(4)	5.1(7)
2315	0.17(1)	15.2(19)
2784	0.148(8)	14.6(17)
2977	0.0046(6)	0.65(9)
3279	0.041(2)	3.3(3)
3427	0.0082(8)	1.1(1)
3921	0.0096(8)	2.2(3)
4147	0.018(1)	5.4(7)
4344	0.0055(6)	1.8(3)
4444	0.0075(7)	3.2(4)
4534[a]	...	0.6(3)
Integrated $L=0$ strength relative to the ground state		$\sum\epsilon_i = 53(3)\%$

[a] We could not determine the cross section for the 4534 keV state at low angles due to the presence of a kinematically broadened light-ion contaminant peak in the region.

identify eight new 0^+ states in ^{136}Ba [55].[2] These results are shown in Fig. 3, together with normalized DWBA cross sections. The data show reasonable agreement with DWUCK4 predictions, except for the well-established 0^+_2 state at 1579 keV [55], where the first minimum occurs at approximately twice the predicted value. This is because of an inherent shortcoming of the DWUCK4 calculations. For example, the calculations ignore multi-step processes and interference from different configurations to the pair transfer amplitude, which can alter the shape of the angular distribution. In Table 2 we list the measured absolute cross sections for these states at $\theta_{lab} = 5^\circ$, in addition to the $L = 0$ transfer strengths to the excited 0^+ states relative to the ground state, denoted by ϵ_i. The latter were determined for each excited state by the product

$$\epsilon_i = \left[\frac{\left(\frac{d\sigma}{d\Omega}\right)^{\text{data}}_{0^+\text{ex}}}{\left(\frac{d\sigma}{d\Omega}\right)^{\text{DWBA}}_{0^+\text{ex}}}\right]_i \left[\frac{\left(\frac{d\sigma}{d\Omega}\right)^{\text{DWBA}}_{\text{G.S.}}}{\left(\frac{d\sigma}{d\Omega}\right)^{\text{data}}_{\text{G.S.}}}\right], \quad (3)$$

which was obtained by normalizing the DWBA calculations to the data at forward angles (where the DWBA is best satisfied) for each plot in Fig. 3 and then taking the ratio of the normalization factor for the 0^+_i state to the ground state normalization factor. This effectively removes the Q-value dependence and other kinematic effects in determining the relative (p,t) strengths.

Our results in Fig. 3 and Table 2 show that in addition to a number of hitherto unknown 0^+ states in ^{136}Ba, we observe a large fragmentation of the $L = 0$, (p,t) strength to these states, with $\sim$ 30% of the ground state strength concentrated at 2.3 and 2.8 MeV. This manifestly indicates a breakdown of the BCS approximation for neutrons in ^{136}Ba [13]. While a similarly large breakdown was not observed in the $^{128-134}$Ba isotopes [42,56,57], such a departure from superfluid behavior in a shape transitional region, particularly around closed shell nuclei, should not be unexpected [13,58]. Our results also indicate that the ground state wavefunctions of ^{138,136}Ba could be largely dissimilar due to the 'non-spherical' nature of the latter. Additionally, the data also present evidence of a small pairing gap in ^{136}Ba, that could occur due to vibrational modes in the pairing field [58,59]. While both possibilities cannot be ruled out, the former will have important ramifications for ^{136}Xe $0\nu\beta\beta$ decay NME calculations. Previous work showed that the static quadrupole moment of the first 2^+ state in ^{136}Ba could be as large as -0.19 or $+0.25$ eb [60–62]. This does not rule out a significantly deformed ^{136}Ba ground state in the context of the NME calculations.

The results from this experiment also allow tests of the nuclear structure models that are used to calculate the NME for ^{136}Xe $0\nu\beta\beta$ decay. We performed one such test using configuration interaction shell model calculations with the NuShellX code [63]. Unlike the DWUCK4 calculations which merely served to identify the observed 0^+ states and determine relative strengths, the shell model calculations were used to assess the absolute (p,t) cross sections, distributed over 0^+ states in ^{136}Ba. The calculations used the five-orbital $(0g_{7/2}, 1d_{5/2}, 1d_{3/2}, 2s_{1/2}, 0h_{11/2})$ valence space for protons and neutrons to determine the wavefunctions for the 0^+ ground state of ^{138}Ba and the lowest fifty 0^+ states in ^{136}Ba. We next used NuShellX to calculate two-neutron transfer amplitudes between these states. The amplitudes were input to the Fresco [64] coupled-reaction channels code, which was used to generate absolute ^{138}Ba(p,t) angular distributions. The Fresco calculations used the same OMP parameters for the proton and triton channels (as described previously) and also took into account the coherent sum of both direct and sequential two-step transfer. The single-nucleon transfer amplitudes for the two-step part were obtained assuming one intermediate state in ^{137}Ba for each of the transferred (n,ℓ,j) values. For the ^{137}Ba-deuteron coupling, we used the global OMP parameters recommended by An and Cai [65], based on a comparison with experimental ^{138}Ba(d,d) angular distribution data that we obtained independently [66].

We used three different Hamiltonians for the calculations, which were corrected for core-polarization due to configuration mixing with orbitals outside the model space [67]. The first Hamiltonian is from Ref. [68] and is called sn100pn in the NuShellX interaction library [63]. The second Hamiltonian (that we call sn100t) is very similar to sn100pn, except with minor modifications and was used in Ref. [12] to calculate $M^{0\nu}$ for ^{136}Xe $\beta\beta$ decay, while the third GCN50:82 [69] Hamiltonian was used by the authors of Ref. [35] to calculate the NME for the decay. Our results are discussed below.

In the left panel of Fig. 4 we present a comparison of the calculated values to our measured angular distribution for the ^{136}Ba ground state. It is apparent that there are significant discrepancies at forward angles, where the maximum deviation is about a factor of two. In the right panel of the same figure, we compare the running sum of our measured and calculated (p,t) cross sections for all 0^+ states at the most forward angle of 5° (where the measured $L = 0$ strength is concentrated). We observe that similar to our experimental results, the calculations predict the (p,t) cross section to be dominated by the transition to the ground state in ^{136}Ba, with smaller contributions from excited 0^+ states. Again, the theory predictions are found to be about a factor of two smaller than the experimental values. What could be causing such an underestimation? It is mainly because the model space for neutrons was limited to only five orbitals near the Fermi surface. Coherent contributions from all orbitals outside the valence space are known to enhance calculated $L = 0$ two-neutron transfer cross sections [70]. We next considered the effects of such core-polarization by calculating ladder-diagram corrections to the two-nucleon transfer amplitudes (TNA), as described in Ref. [70], assuming the scattering of pairs of neutrons to twenty three orbitals beyond the model space (up to $i_{11/2}$). As shown in Fig. 5, the revised calculations that incorporated the core-polarization effects show enhancements in the predicted cross sections by about a factor of 1.5, and agree with experiment to $\sim$ 22% for the GCN50:82 Hamiltonian and $\sim$ 14% for the others. The predicted relative cross sections over the 0^+

[2] We ignore the $E_x = 2141$ keV [55] state in our analysis as it overlaps with a $J^\pi = 5^-$ state at 2140 keV. Our measured angular distribution for this peak is consistent with a $L = 5$ transfer, implying that the 0^+ state is weakly populated.

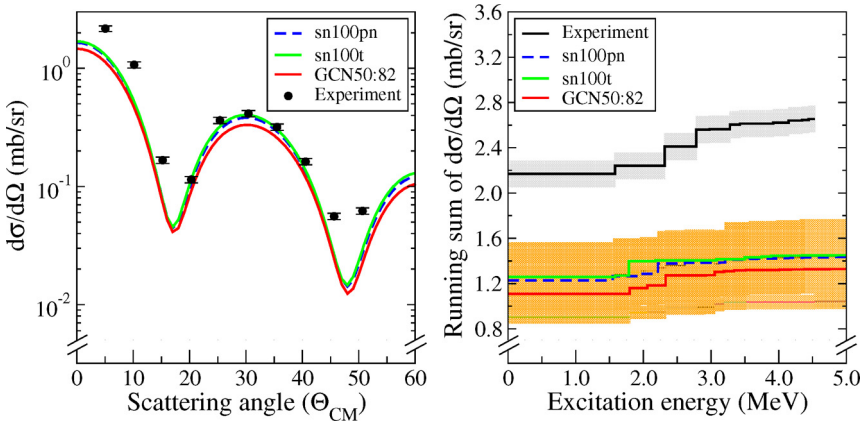

Fig. 4. Left panel: Measured ground state ^{138}Ba(p,t) cross sections overlayed with absolute values obtained from the shell model/Fresco calculations described in the text. Right panel: Running sum of experimental (p,t) cross sections at $\theta_{\rm lab} = 5°$, compared with the calculated values. The grey band represents the experimental uncertainties from Table 2. The orange band includes a 10% uncertainty due to multi-step contributions and an overly conservative spread arising from the use for different OMP parameters in the DWBA analysis. The latter dominates the total uncertainty.

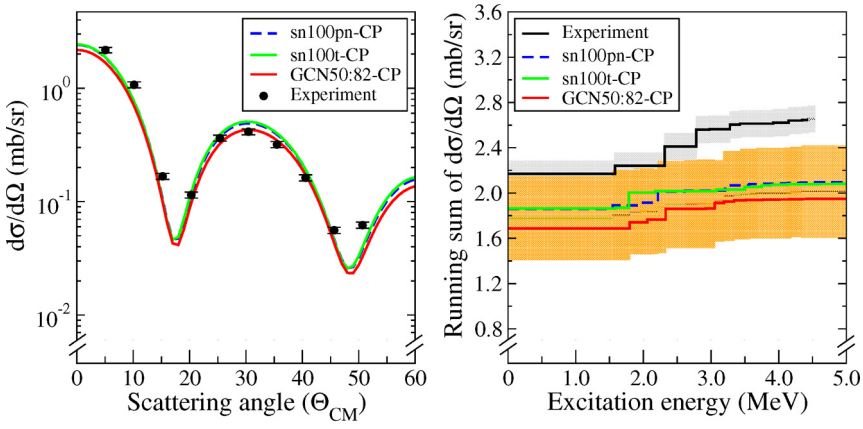

Fig. 5. Left panel: Measured ground state ^{138}Ba(p,t) cross sections overlayed with absolute values obtained from shell model/Fresco calculations that incorporated core-polarization corrections as described in the text. Right panel: Running sum of experimental (p,t) cross sections at $\theta_{\rm lab} = 5°$, compared with calculated values obtained after core-polarization effects are taken into account. The uncertainty bands are the same as described in the caption for Fig. 4.

states are also found to agree reasonably well with experiment, particularly for the GCN50:82 Hamiltonian. This agreement did not significantly improve on making small adjustments of the single-particle energies and pairing strengths of the Hamiltonians.

In the final part of our analysis we used these results to benchmark NME calculations for ^{136}Xe $0\nu\beta\beta$ decay. This was based on the arguments presented in Ref. [71], where it was shown that the $0\nu\beta\beta$ decay NME for a parent nucleus with mass number A can be expanded as a sum over states in an intermediate nucleus with mass number $(A-2)$. For the case of ^{136}Xe, one can similarly evaluate the NME by summing over the products of the TNA for two-neutron removal to ^{134}Xe, the TNA for two-proton addition to ^{136}Ba, and the two-body matrix element for the double-beta decay operators (cf. Eq. (9) in Ref. [71]). The most significant contribution to the NME is through the 0^+ ground state in the ^{134}Xe, while $J > 0$ intermediate states mainly cancel the $\Delta J = 0$ term [71]. This is similar to other calculations [35,72] that separate the NME in terms of nucleon pairs coupled to angular momentum and parity $J^\pi = 0^+$ and $J^\pi \neq 0^+$, where the $J > 0$ contributions predominantly cancel the leading $J^\pi = 0^+$ term (see Fig. 1 in Ref. [35]).

The ^{136}Xe $\rightarrow$ ^{134}Xe transition described above is expected to be very similar to ^{138}Ba $\rightarrow$ ^{136}Ba. This is because both ^{136}Xe and ^{138}Ba are singly closed shell, nearly spherical nuclei at $N = 82$. Furthermore, theory calculations predict the ^{134}Xe and ^{136}Ba ground states to have similar structure [40]. This is supported by strong empirical evidence. If we examine the low-lying levels in these nuclei, their 2^+_1 states have very similar excitation energies and $B(E2;\uparrow)$ values [73]. Additional comparison, after including recent results from $(n,n'\gamma)$ experimental work [74], shows that the energies of the 2^+_2, 2^+_3, 0^+_2, 4^+_1, 4^+_2 and 7^-_1 states are also very similar in both nuclei. Therefore, the low-lying level schemes in ^{134}Xe and ^{136}Ba are nearly identical. This similarity allows a benchmarking of ^{136}Xe $0\nu\beta\beta$ decay NME calculations using our ^{138}Ba(p,t) data. As described below, on the basis of this benchmarking we can evaluate a revised value for the dominant $J^\pi = 0^+$ Gamow-Teller (GT) component of the NME. This is done by first calculating the NME through the $J^\pi = 0^+$ ground state in ^{134}Xe, both with and without the core-polarization corrections to the TNA. For the former we chose expanded sets of TNA, for both (neutron removal and proton addition) parts of the calculation, with the $2n$ removal part being the one that better reproduces our measured ^{138}Ba(p,t) cross section. The ratio of the results was determined to be $R = 1.58$, which is the expected enhancement in the NME due to core-polarization. Next we performed a more rigorous five-orbital valence space ISM calculation of the NME (for light neutrino exchange) with the sn100t Hamiltonian, as in Ref. [12]. On using the CD-Bonn potential [75] for two-nucleon short range correlations (SRC) and further including higher-order contributions (HOC) due to induced nucleon currents [76], we determine the matrix element to be $M^{0\nu}_{GT}(J^\pi = 0^+) = 5.67$. Finally, on incorporating the above enhancement due to core-polarization effects, we revise the NME to $M^{0\nu}_{GT}(J^\pi = 0^+) = R \times 5.67 = 8.96$.

To make further comparisons, we also performed a large-scale spherical QRPA calculation of the NME (with HOC and the CD-Bonn SRC), using the model parameters of Ref. [23] and 28 orbitals for major oscillator shells with $N \leq 6$. This resulted in a value $M^{0\nu}_{GT}(J^{\pi} = 0^{+}) = 9.63$. It is reassuring that both our QRPA and (revised) shell model results for the NME are now very similar in value. Clearly, previous configuration interaction (ISM) calculations [35] had underestimated the $J = 0$ component of the Gamow-Teller NME. It is expected that the $J > 0$ cancellations would also increase due to similar core-polarization effects. We therefore recommend improved calculations of both the $J = 0$ part of NME as well as the canceling $M^{0\nu}_{GT}(J > 0)$ term. These can be done along the lines of a many-body perturbation theory treatment [77] or $V_{\text{low}-k}$/IMSRG based effective Hamiltonians and transition operators [78,79], that take into account physics contributions from beyond the model space. Since the details of the cancellation between the $J = 0$ and $J > 0$ contributions to the NME are model dependent, our result also serves to benchmark such future calculations. We note that in order to make the connection with two-nucleon transfer reaction data, it is important that the results of these calculations be expressed in terms of their J^{π} decomposition.

In summary, this work demonstrates for the first time an evaluation of part of a $0\nu\beta\beta$ decay NME using experimental data. In addition to providing a benchmark for future calculations, it also presents a new avenue of approach for evaluating $0\nu\beta\beta$ decay NMEs more accurately, motivating similar investigations in other candidates. We also report for the first time a large breakdown of the neutron BCS approximation in an even barium nucleus with $N \leq 82$. Our observations motivate a reassessment of the neutron pairing approximation in ^{136}Ba, used in some NME calculations for ^{136}Xe $0\nu\beta\beta$ decay and invite further investigations of the shape of ^{136}Ba.

Declaration of competing interest

The authors declare that they have no known competing financial interests or personal relationships that could have appeared to influence the work reported in this paper.

Acknowledgements

We are grateful to Ian Thompson for his assistance with the Fresco calculations. This work was partially supported by the National Research Foundation (NRF) of South Africa, under Grant No. 85100, the Natural Sciences and Engineering Research Council of Canada (NSERC), The U.S. National Science Foundation under Grant No. PHY-1811855 and The U.S. Department of Energy, Office of Science under Grant Nos. DE-SC0017649 and DE-SC0015376. P.A. acknowledges funding from the Claude Leon Foundation in the form of a postdoctoral fellowship.

References

[1] J.J. Sakurai, Invariance Principles and Elementary Particles, Princeton University Press, 1965.
[2] Frank T. Avignone III, Steven R. Elliott, Jonathan Engel, Double beta decay, Majorana neutrinos, and neutrino mass, Rev. Mod. Phys. 80 (2008) 481–516, https://doi.org/10.1103/RevModPhys.80.481.
[3] S.M. Bilenky, C. Giunti, Neutrinoless double-beta decay: a probe of physics beyond the standard model, Int. J. Mod. Phys. A 30 (04n05) (2015) 1530001.
[4] M.J. Dolinski, A.W. Poon, W. Rodejohann, Neutrinoless double-beta decay: status and prospects, Annu. Rev. Nucl. Part. Sci. 69 (1) (2019) 219, https://doi.org/10.1146/annurev-nucl-101918-023407.
[5] Werner Rodejohann, Neutrinoless double beta decay and particle physics, Int. J. Mod. Phys. E 20 (2011) 1833.
[6] Ziro Maki, Masami Nakagawa, Shoichi Sakata, Remarks on the unified model of elementary particles, Prog. Theor. Phys. 28 (5) (1962) 870–880, https://doi.org/10.1143/PTP.28.870.
[7] B. Pontecorvo, Sov. Phys. JETP 26 (5) (1968) 984.
[8] S.M. Bilenky, A. Faessler, T. Gutsche, F. Šimkovic, Neutrinoless double β-decay and neutrino mass hierarchies, Phys. Rev. D 72 (2005) 053015, https://doi.org/10.1103/PhysRevD.72.053015.
[9] S. Pascoli, S. Petcov, W. Rodejohann, On the CP violation associated with Majorana neutrinos and neutrinoless double-beta decay, Phys. Lett. B 549 (1) (2002) 177–193, https://doi.org/10.1016/S0370-2693(02)02852-6, http://www.sciencedirect.com/science/article/pii/S0370269302028526.
[10] J.D. Vergados, H. Ejiri, F. Šimkovic, Neutrinoless double beta decay and neutrino mass, Int. J. Mod. Phys. E 25 (2016) 1630007.
[11] Jonathan Engel, Javier Menéndez, Status and future of nuclear matrix elements for neutrinoless double-beta decay: a review, Rep. Prog. Phys. 80 (4) (2017) 046301.
[12] M. Horoi, B.A. Brown, Shell-model analysis of the ^{136}Xe double beta decay nuclear matrix elements, Phys. Rev. Lett. 110 (2013) 222502, https://doi.org/10.1103/PhysRevLett.110.222502.
[13] S.J. Freeman, J.P. Schiffer, Constraining the $0\nu2\beta$ matrix elements by nuclear structure observables, J. Phys. G, Nucl. Part. Phys. 39 (12) (2012) 124004.
[14] D. Frekers, M. Alanssari, Charge-exchange reactions and the quest for resolution, Eur. Phys. J. A 54 (10) (2018) 177.
[15] P. Pirinen, J. Suhonen, Systematic approach to β and $2\nu\beta\beta$ decays of mass $A = 100$–136 nuclei, Phys. Rev. C 91 (2015) 054309, https://doi.org/10.1103/PhysRevC.91.054309.
[16] T.R. Rodríguez, G. Martínez-Pinedo, Energy density functional study of nuclear matrix elements for neutrinoless $\beta\beta$ decay, Phys. Rev. Lett. 105 (2010) 252503, https://doi.org/10.1103/PhysRevLett.105.252503.
[17] J. Menéndez, A. Poves, E. Caurier, F. Nowacki, Occupancies of individual orbits, and the nuclear matrix element of the ^{76}Ge neutrinoless $\beta\beta$ decay, Phys. Rev. C 80 (2009) 048501, https://doi.org/10.1103/PhysRevC.80.048501.
[18] R. Saakyan, Two-neutrino double-beta decay, Annu. Rev. Nucl. Part. Sci. 63 (1) (2013) 503–529, https://doi.org/10.1146/annurev-nucl-102711-094904.
[19] A. Gando, et al., Search for Majorana neutrinos near the inverted mass hierarchy region with KamLAND-Zen, Phys. Rev. Lett. 117 (2016) 082503, https://doi.org/10.1103/PhysRevLett.117.082503.
[20] D.-L. Fang, A. Faessler, F. Šimkovic, $0\nu\beta\beta$-decay nuclear matrix element for light and heavy neutrino mass mechanisms from deformed quasiparticle random-phase approximation calculations for ^{76}Ge,^{82} Se,^{130} Te,^{136} Xe, and ^{150}Nd with isospin restoration, Phys. Rev. C 97 (2018) 045503, https://doi.org/10.1103/PhysRevC.97.045503.
[21] J. Hyvärinen, J. Suhonen, Nuclear matrix elements for $0\nu\beta\beta$ decays with light or heavy Majorana-neutrino exchange, Phys. Rev. C 91 (2015) 024613, https://doi.org/10.1103/PhysRevC.91.024613.
[22] M.T. Mustonen, J. Engel, Large-scale calculations of the double-β decay of ^{76}Ge, ^{130}Te, ^{136}Xe, and ^{150}Nd in the deformed self-consistent skyrme quasiparticle random-phase approximation, Phys. Rev. C 87 (2013) 064302, https://doi.org/10.1103/PhysRevC.87.064302.
[23] F. Šimkovic, V. Rodin, A. Faessler, P. Vogel, $0\nu\beta\beta$ and $2\nu\beta\beta$ nuclear matrix elements, quasiparticle random-phase approximation, and isospin symmetry restoration, Phys. Rev. C 87 (2013) 045501, https://doi.org/10.1103/PhysRevC.87.045501.
[24] J. Menéndez, A. Poves, E. Caurier, F. Nowacki, Disassembling the nuclear matrix elements of the neutrinoless decay, Nucl. Phys. A 818 (3) (2009) 139–151, https://doi.org/10.1016/j.nuclphysa.2008.12.005, http://www.sciencedirect.com/science/article/pii/S0375947408008233.
[25] L.S. Song, J.M. Yao, P. Ring, J. Meng, Nuclear matrix element of neutrinoless double-β decay: relativity and short-range correlations, Phys. Rev. C 95 (2017) 024305, https://doi.org/10.1103/PhysRevC.95.024305.
[26] N.L. Vaquero, T.R. Rodríguez, J.L. Egido, Shape and pairing fluctuation effects on neutrinoless double beta decay nuclear matrix elements, Phys. Rev. Lett. 111 (2013) 142501, https://doi.org/10.1103/PhysRevLett.111.142501.
[27] J. Barea, J. Kotila, F. Iachello, $0\nu\beta\beta$ and $2\nu\beta\beta$ nuclear matrix elements in the interacting boson model with isospin restoration, Phys. Rev. C 91 (2015) 034304, https://doi.org/10.1103/PhysRevC.91.034304.
[28] C.F. Jiao, M. Horoi, A. Neacsu, Neutrinoless double-β decay of ^{124}Sn, ^{130}Te, and ^{136}Xe in the Hamiltonian-based generator-coordinate method, Phys. Rev. C 98 (2018) 064324, https://doi.org/10.1103/PhysRevC.98.064324.
[29] J.B. Albert, et al., Sensitivity and discovery potential of the proposed nEXO experiment to neutrinoless double-β decay, Phys. Rev. C 97 (2018) 065503, https://doi.org/10.1103/PhysRevC.97.065503.
[30] A.D. McDonald, et al., Demonstration of single-barium-ion sensitivity for neutrinoless double-beta decay using single-molecule fluorescence imaging, Phys. Rev. Lett. 120 (2018) 132504, https://doi.org/10.1103/PhysRevLett.120.132504.
[31] S. Pascoli, S.T. Petcov, T. Schwetz, The absolute neutrino mass scale, neutrino mass spectrum, Majorana CP-violation and neutrinoless double-beta decay, Nucl. Phys. B 734 (1) (2006) 24–49, https://doi.org/10.1016/j.nuclphysb.2005.11.003, http://www.sciencedirect.com/science/article/pii/S0550321305009739.
[32] M. Fukugita, T. Yanagida, Baryogenesis without grand unification, Phys. Lett. B 174 (1) (1986) 45–47, https://doi.org/10.1016/0370-2693(86)91126-3, http://www.sciencedirect.com/science/article/pii/0370269386911263.

[33] S. Pascoli, S.T. Petcov, A. Riotto, Connecting low energy leptonic CP violation to leptogenesis, Phys. Rev. D 75 (2007) 083511, https://doi.org/10.1103/PhysRevD.75.083511.

[34] K. Moffat, S. Pascoli, S.T. Petcov, J. Turner, Leptogenesis from low energy CP violation, J. High Energy Phys. 2019 (3) (2019) 34, https://doi.org/10.1007/JHEP03(2019)034.

[35] E. Caurier, J. Menéndez, F. Nowacki, A. Poves, Influence of pairing on the nuclear matrix elements of the neutrinoless $\beta\beta$ decays, Phys. Rev. Lett. 100 (2008) 052503, https://doi.org/10.1103/PhysRevLett.100.052503.

[36] J. Menéndez, T.R. Rodríguez, G. Martínez-Pinedo, A. Poves, Correlations and neutrinoless $\beta\beta$ decay nuclear matrix elements of pf-shell nuclei, Phys. Rev. C 90 (2014) 024311, https://doi.org/10.1103/PhysRevC.90.024311.

[37] J. Menéndez, N. Hinohara, J. Engel, G. Martínez-Pinedo, T.R. Rodríguez, Testing the importance of collective correlations in neutrinoless $\beta\beta$ decay, Phys. Rev. C 93 (2016) 014305, https://doi.org/10.1103/PhysRevC.93.014305.

[38] J.P. Entwisle, et al., Change of nuclear configurations in the neutrinoless double-β decay of ^{130}Te $\rightarrow^{130}$ Xe and ^{136}Xe $\rightarrow^{136}$ Ba, Phys. Rev. C 93 (2016) 064312, https://doi.org/10.1103/PhysRevC.93.064312.

[39] S.V. Szwec, et al., Rearrangement of valence neutrons in the neutrinoless double-β decay of ^{136}Xe, Phys. Rev. C 94 (2016) 054314, https://doi.org/10.1103/PhysRevC.94.054314.

[40] E. Marshalek, L.W. Person, R.K. Sheline, Systematics of deformations of atomic nuclei, Rev. Mod. Phys. 35 (1963) 108–116, https://doi.org/10.1103/RevModPhys.35.108.

[41] H. Kusakari, K. Kitao, S. Kono, Y. Ishizaki, Study of even-mass Ba nuclei by the (p,t) reaction, Nucl. Phys. A 341 (2) (1980) 206–218, https://doi.org/10.1016/0375-9474(80)90309-7, http://www.sciencedirect.com/science/article/pii/0375947480903097.

[42] S. Pascu, et al., Structure investigation with the (p,t) reaction on ^{132,134}Ba nuclei, Phys. Rev. C 81 (2010) 014304, https://doi.org/10.1103/PhysRevC.81.014304.

[43] M. Löffler, H. Scheerer, H. Vonach, The ion optical properties of the Munich Q3D-spectrograph investigated by means of a special experimental ray tracing method, Nucl. Instrum. Methods 111 (1) (1973) 1–12, https://doi.org/10.1016/0029-554X(73)90090-6, http://www.sciencedirect.com/science/article/pii/0029554X73900906.

[44] G. Dollinger, T. Faestermann, Physics at the Munich tandem accelerator laboratory, Nucl. Phys. News 28 (1) (2018) 5–12, https://doi.org/10.1080/10619127.2018.1427405.

[45] F.D. Becchetti, G.W. Greenlees, Nucleon-nucleus optical-model parameters, $A > 40$, $E < 50$ MeV, Phys. Rev. 182 (1969) 1190–1209, https://doi.org/10.1103/PhysRev.182.1190.

[46] A. Koning, J. Delaroche, Local and global nucleon optical models from 1 keV to 200 MeV, Nucl. Phys. A 713 (3) (2003) 231–310, https://doi.org/10.1016/S0375-9474(02)01321-0, http://www.sciencedirect.com/science/article/pii/S0375947402013210.

[47] J.J.H. Menet, E.E. Gross, J.J. Malanify, A. Zucker, Total-reaction-cross-section measurements for 30-60-MeV protons and the imaginary optical potential, Phys. Rev. C 4 (1971) 1114–1129, https://doi.org/10.1103/PhysRevC.4.1114.

[48] Richard L. Walter, Paul P. Guss, A global optical model for neutron scattering for $A > 53$ and 10 MeV $< E <$ 80 MeV, Radiat. Eff. 95 (1–4) (1986) 73–84, https://doi.org/10.1080/00337578608208670.

[49] R. Varner, W. Thompson, T. McAbee, E. Ludwig, T. Clegg, A global nucleon optical model potential, Phys. Rep. 201 (2) (1991) 57–119, https://doi.org/10.1016/0370-1573(91)90039-O, http://www.sciencedirect.com/science/article/pii/037015739190039O.

[50] P.D. Kunz, DWUCK4 DWBA Program, University of Colorado, 1978, unpublished.

[51] X. Li, C. Liang, C. Cai, Global triton optical model potential, Nucl. Phys. A 789 (1) (2007) 103–113, https://doi.org/10.1016/j.nuclphysa.2007.03.004, http://www.sciencedirect.com/science/article/pii/S0375947407002291.

[52] F.D. Becchetti, G.W. Greenlees, Nucleon-nucleus optical-model parameters, $A > 40$, $E < 50$ MeV, Phys. Rev. 182 (1969) 1190–1209, https://doi.org/10.1103/PhysRev.182.1190.

[53] P.T. Deason, C.H. King, T.L. Khoo, J.A. Nolen, F.M. Bernthal, ^{194,196,198}Pt(p,t) reactions at 35 MeV, Phys. Rev. C 20 (1979) 927–943, https://doi.org/10.1103/PhysRevC.20.927.

[54] B.M. Rebeiro, in preparation.

[55] E. Mccutchan, Nuclear data sheets for $A = 136$, Nucl. Data Sheets 152 (2018) 331–667, https://doi.org/10.1016/j.nds.2018.10.002, http://www.sciencedirect.com/science/article/pii/S0090375218300711.

[56] S. Pascu, G.C. ăta Danil, D. Bucurescu, N. Mărginean, N.V. Zamfir, G. Graw, A. Gollwitzer, D. Hofer, B.D. Valnion, Investigation of the ^{128}Ba nucleus with the (p,t) reaction, Phys. Rev. C 79 (2009) 064323, https://doi.org/10.1103/PhysRevC.79.064323.

[57] G. Suliman, D. Bucurescu, R. Hertenberger, H.F. Wirth, T. Faestermann, R. Krücken, T. Behrens, V. Bildstein, K. Eppinger, C. Hinke, M. Mahgoub, P. Meierbeck, M. Reithner, S. Schwertel, N. Chauvin, Study of the ^{130}Ba nucleus with the (p,t) reaction, Eur. Phys. J. A 36 (3) (2008) 243–250, https://doi.org/10.1140/epja/i2008-10589-2.

[58] R.A. Broglia, O. Hansen, C. Riedel, Two-Neutron Transfer Reactions and the Pairing Model, Springer US, Boston, MA, 1973, pp. 287–457.

[59] D.M. Brink, R.A. Broglia, Nuclear Superfluidity, Cambridge University Press, 2010.

[60] J.R. Kerns, J.X. Saladin, Reorientation effect measurements on Ba^{134,136,138}, Phys. Rev. C 6 (1972) 1016–1023, https://doi.org/10.1103/PhysRevC.6.1016.

[61] M.J. Bechara, O. Dietzsch, J.H. Hirata, Quadrupole moment of the first 2^+ excited state in ^{136}Ba through the reorientation effect, Phys. Rev. C 29 (1984) 1672–1677, https://doi.org/10.1103/PhysRevC.29.1672.

[62] P.J. Rothschild, A.M. Baxter, S.M. Burnett, M.P. Fewell, G.J. Gyapong, R.H. Spear, Quadrupole moment of the first excited state of ^{136}Ba, Phys. Rev. C 34 (1986) 732–735, https://doi.org/10.1103/PhysRevC.34.732.

[63] B.A. Brown, W.D.M. Rae, The shell-model code NuShellX@MSU, Nucl. Data Sheets 120 (2014) 115–118, https://doi.org/10.1016/j.nds.2014.07.022, http://www.sciencedirect.com/science/article/pii/S0090375214004748.

[64] http://www.fresco.org.uk/index.htm.

[65] H. An, C. Cai, Global deuteron optical model potential for the energy range up to 183 MeV, Phys. Rev. C 73 (2006) 054605, https://doi.org/10.1103/PhysRevC.73.054605.

[66] B. Rebeiro, Nuclear structure studies in the A = 136 region using transfer reactions, Ph.D. thesis, University of the Western Cape, 2018, https://etd.uwc.ac.za/handle/11394/6759.

[67] Morten Hjorth-Jensen, Thomas T.S. Kuo, Eivind Osnes, Realistic effective interactions for nuclear systems, Phys. Rep. 261 (3) (1995) 125–270, https://doi.org/10.1016/0370-1573(95)00012-6, http://www.sciencedirect.com/science/article/pii/0370157395000126.

[68] B.A. Brown, N.J. Stone, J.R. Stone, I.S. Towner, M. Hjorth-Jensen, Magnetic moments of the 2_1^+ states around ^{132}Sn, Phys. Rev. C 71 (2005) 044317, https://doi.org/10.1103/PhysRevC.71.044317.

[69] E. Caurier, F. Nowacki, A. Poves, K. Sieja, Collectivity in the light xenon isotopes: a shell model study, Phys. Rev. C 82 (2010) 064304, https://doi.org/10.1103/PhysRevC.82.064304.

[70] P. Decowski, W. Benenson, B.A. Brown, H. Nann, Levels of ^{52}Fe studied with the (p,t) reaction, Nucl. Phys. A 302 (1) (1978) 186–204, https://doi.org/10.1016/0375-9474(78)90294-4, http://www.sciencedirect.com/science/article/pii/0375947478902944.

[71] B.A. Brown, M. Horoi, R.A. Sen'kov, Nuclear structure aspects of neutrinoless double-β decay, Phys. Rev. Lett. 113 (2014) 262501, https://doi.org/10.1103/PhysRevLett.113.262501.

[72] J. Menéndez, Neutrinoless $\beta\beta$ decay mediated by the exchange of light and heavy neutrinos: the role of nuclear structure correlations, J. Phys. G, Nucl. Part. Phys. 45 (1) (2017) 014003, https://doi.org/10.1088/1361-6471/aa9bd4.

[73] https://www.nndc.bnl.gov/ensdf/.

[74] E.E. Peters, A. Chakraborty, B.P. Crider, S.F. Ashley, E. Elhami, S.F. Hicks, A. Kumar, M.T. McEllistrem, S. Mukhopadhyay, J.N. Orce, F.M. Prados-Estévez, S.W. Yates, Level lifetimes and the structure of ^{134}Xe from inelastic neutron scattering, Phys. Rev. C 96 (2017) 014313, https://doi.org/10.1103/PhysRevC.96.014313.

[75] R. Machleidt, F. Sammarruca, Y. Song, Nonlocal nature of the nuclear force and its impact on nuclear structure, Phys. Rev. C 53 (1996) R1483–R1487, https://doi.org/10.1103/PhysRevC.53.R1483.

[76] F. Šimkovic, G. Pantis, J.D. Vergados, A. Faessler, Additional nucleon current contributions to neutrinoless double β decay, Phys. Rev. C 60 (1999) 055502, https://doi.org/10.1103/PhysRevC.60.055502.

[77] J.D. Holt, J. Engel, Effective double-β-decay operator for ^{76}Ge and ^{82}Se, Phys. Rev. C 87 (2013) 064315, https://doi.org/10.1103/PhysRevC.87.064315.

[78] L. Coraggio, A. Gargano, N. Itaco, R. Mancino, F. Nowacki, Calculation of the neutrinoless double-β decay matrix element within the realistic shell model, Phys. Rev. C 101 (2020) 044315, https://doi.org/10.1103/PhysRevC.101.044315.

[79] J.M. Yao, B. Bally, J. Engel, R. Wirth, T.R. Rodríguez, H. Hergert, Ab initio treatment of collective correlations and the neutrinoless double beta decay of ^{48}Ca, Phys. Rev. Lett. 124 (2020) 232501, https://doi.org/10.1103/PhysRevLett.124.232501.